Review

Herbert Meier*

Extended conjugation in stilbenoid squaraines

https://doi.org/10.1515/znb-2018-0260
Received December 12, 2018; accepted January 15, 2019

Abstract: Squaraines, two-fold condensation products in 1,3-position of squaric acid, represent dyes or pigments of high actuality. After their first boom in electrophotography diverse applications are presently studied in a wide area of research, which reaches from electrooptical materials to biosensors and compounds used in photodynamic therapy. Absorption and/or emission ranges in the NIR are mandatory for many of these techniques. The present article deals with stilbenoid squaraines, which feature an extended conjugation in their biradicaloid D-π-A-π-D structure. Due to the charge-transfer character of the excitation, boundaries are set for the optimal length of the conjugation. The absorption maxima of the stilbenoid squaraines and their aggregates are lying in chloroform as a solvent between 600 and 1000 nm. In the solid state panchromatic absorptions can be observed, which reach far into the NIR region. The facile preparation of squaraines bearing stilbene building blocks in one or two of their arms and moreover the easy access to dyes with multiple squaraine units fixed to stilbenoid scaffolds promise a wide palette of further applications in materials science.

Keywords: aggregation; conjugation; NIR dyes; squaraines; stilbenes.

1 Introduction

Soon after their first syntheses [1, 2] squaraines (**1**) reached a great significance as bright violet, blue or blue-green dyes or pigments [3–16]. Their primary boom in electrophotography (xerography) [7] was soon ensued by many diverse applications. The following, partly overlapping topics shall be outlined here:

- semiconductive or photoconductive electrooptical materials [9, 16–19],
- materials in field-effect transistors [8, 19–22],
- pigments in solar cells [9, 14, 23–30],
- materials for non-linear optics (NLO) [9, 31–33],
- two-photon absorbing compounds [9, 34, 35],
- NIR emitting fluorescent dyes [36–39],
- materials used for fluorescence imaging [13, 40–49],
- biosensors [9, 12, 50, 51],
- compounds for photodynamic therapy (PDT) [9, 12, 35, 52–55].

Figure 1 shows the canonical representations of 1,3-diarylsquaraines (**1**). The name squaraine for such derivatives of squaric acid was first suggested by A. H. Schmidt [56]. These inner salts (betaines) can be described by resonance structures, which contain a positive charge in the four-membered ring and a negative charge on one of the exocyclic oxygen atoms. Within this article the core is drawn by a cross-conjugated cyclobutenediylium diolate structure bearing a +2 charge in the aromatic four-membered ring and a –1 charge on both exocyclic oxygen atoms. However, the delocalization of the positive charge into the lateral aryl substituents in 1,3-position is important for the stability of the squaraines. 1,3-Diphenylsquaraine for example is not sufficiently stable. At least one phenyl substituent R must have an electron-donating character.

The singlet biradical structure of **1** (Fig. 1) was underestimated for a long time in favor of the quadrupolar donor-acceptor-donor (D-π-A-π-D) structure. The results of more recent calculations indicate a coupling between the mesoionic and the biradical form and assign a biradicaloid character to the 1,3-diarylsquaraines (**1**) [57–61].

1,3-Diarylsquaraines (**1**) exhibit an intense absorption of visible light. 1,3-Bis[4-(dimethylamino)phenyl]squaraine (**1a**) [2] represents a typical example.

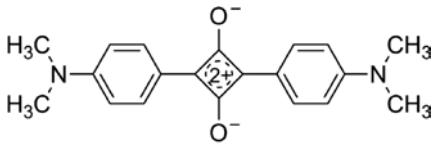

1a (D_{2h})

The strong, narrow long-wavelength absorption band ($\lambda_{max} = 624$ nm, $\varepsilon_{max} = 10^{5.43}$ L mol^{-1} cm^{-1} in $CHCl_3$) [62] corresponds to a π→π* transition (HOMO→LUMO)

***Corresponding author: Herbert Meier,** Institute of Organic Chemistry, University of Mainz, Duesbergweg 10–14, D-55099 Mainz, Germany, e-mail: hmeier@uni-mainz.de

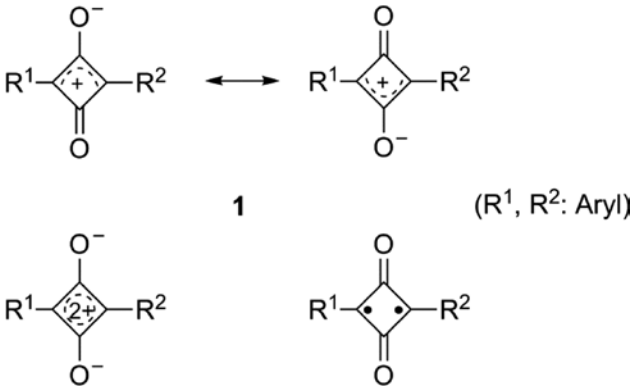

Fig. 1: Canonical structures of 1,3-diarylsquaraines **1**.

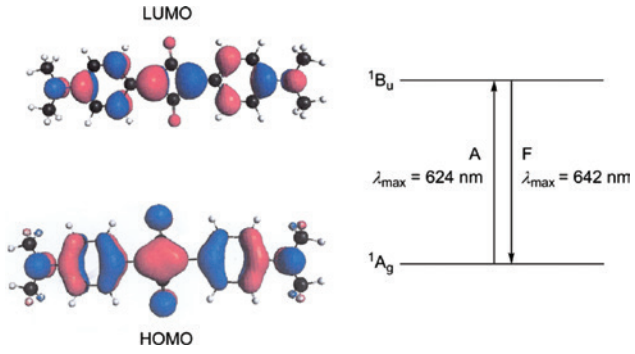

Fig. 2: Frontier orbitals of 1,3-bis(4-dimethylaminophenyl) squaraine (**1a**) and long-wavelength electron transition (absorption and emission in CH_2Cl_2) [63, 64, 67].

which arises predominantly from the core (Fig. 2) [63–65]. The charge-transfer character of the band is small ($q^{CT} = 0.25$ e) as calculated by the SAC-CI method, which gives in this case better results than the TD-DFT method [57]. The first excited singlet state gives rise to a strong fluorescence ($\lambda_{max} = 642$ nm, quantum yield $\phi_F = 0.70$). The fluorescence lifetime amounts to 1.27 ns in $CHCl_3$ at room temperature [64]. Embedded in PPMA, the absorption of the molecule becomes panchromatic with $\phi_F = 0.65$ [66].

The quadrupole character of **1a** is responsible for the formation of aggregates [68, 69]. In many UV/Vis/NIR spectra of squaraines, absorptions of monomers, dimers and higher aggregates up to hexamers are superimposed.

Extension of the conjugation in these D-π-A-π-D systems should shift the absorption and fluorescence far into the NIR region. This argument is also valid for the biradical structure. An intense absorption and/or fluorescence in the NIR is mandatory for many applications of squaraines.

Vinylene or 1,4-phenylenevinylene segments in the lateral substituents (arms) seem to be suitable for this

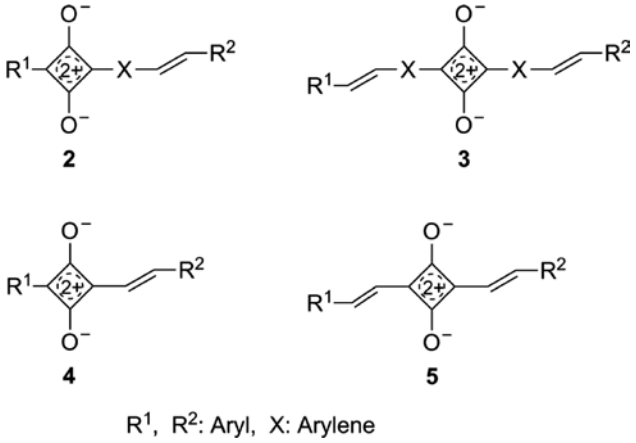

Fig. 3: Possible extension of conjugation in 1,3-diarylsquaraines (**1**) to 1-aryl-3-stilbenylsquaraines (**2**), 1,3-distilbenylsquaraines (**3**) or 1-aryl-3-styrylsquaraines (**4**), and 1,3-distyrylsquaraines (**5**).

purpose. Thus, the structures **2–5** in Fig. 3 were conceived as target structures for dyes which absorb and fluoresce in the NIR. Stilbene units, which are present in the structures of type **2** and **3**, are important building blocks in many compounds used in materials science [70, 71].

Whereas a large number of squaraines **2** and **3** were synthesized, only a single copper complex **4a** [72] of a 1-aryl-3-styrylsquaraine (**4**) has been described and 1,3-distyrylsquaraines (**5**) were only included in theoretical studies [73].

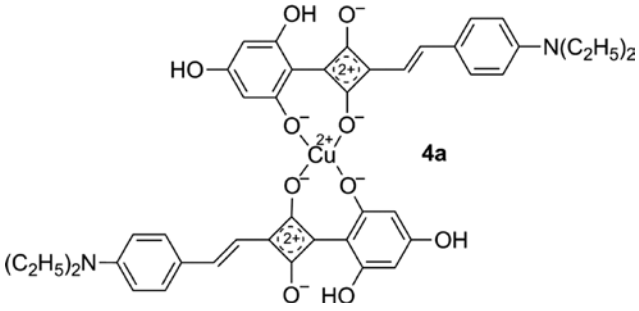

Nevertheless, many squaraines **4′** and **5′** were synthesized which bear one or two heterocyclic substituents, with R^1 or R^2 or both featuring thiophene, thiadiazole, thiatriazole, pyridine or condensed heterocyclic ring systems [9, 15, 74].

2 1-Aryl-3-stilbenylsquaraines

The preparation of 1-aryl-3-stilbenylsquaraines (**2**) is shown in Schemes 1 and 2.

Squaric acid dimethyl ester (**6**) reacts with the *trans*-stilbene derivatives **7** to yield the semisquaric acids **8**

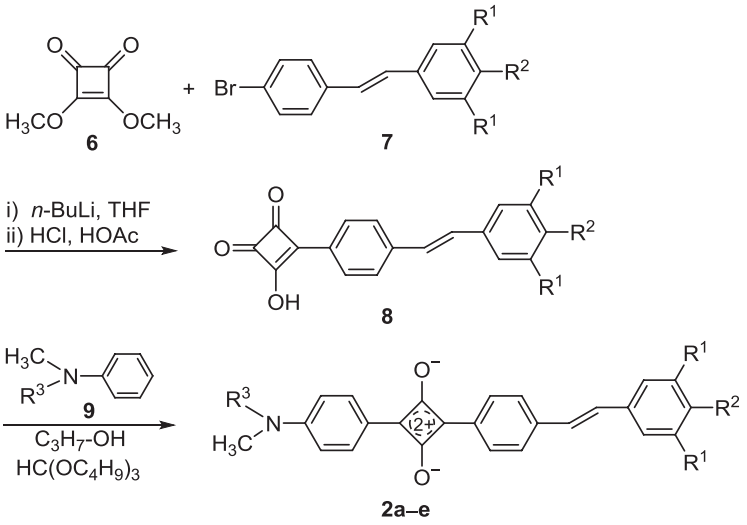

6 7 8 9 2a–e

2	R^1	R^2	R^3	Yield (%) 8 → 2	M. p. (°C)[a]	λ_{max} (nm)[b]	Ref.
a	H	OCH_3	CH_3	64	247	627	75, 76
b	H	OC_3H_7	CH_3	48	254	626	76
c	H	OC_6H_{13}	CH_3	69	243	627	75, 76
d	OC_3H_7	H	CH_3	26	235	614	76
e	OC_3H_7	OC_3H_7	$(CH_2)_6$-OH	4–9	260	626	76

[a] Decomposition; [b] in chloroform

Scheme 1: Preparation of the 1-alkyl-3-stilbenylsquaraines **2a–e.**

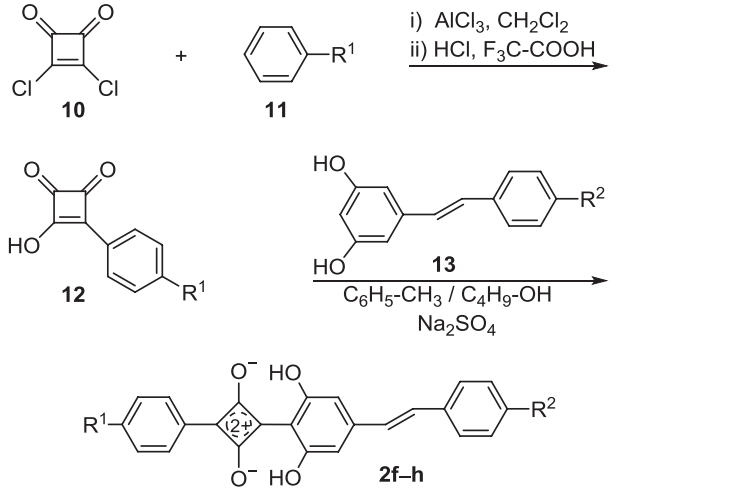

10 11 12 13 2f–h

2	R^1	R^2	Yield (%) 13 → 2	M. p. (°C)	λ_{max} (nm)[a]	Ref.
f	H	$N[CH_2\text{-}CH(C_6H_{13})_2]_2$	43	173	674	79
g	$N[CH_2\text{-}CH(C_6H_{13})_2]_2$	$N[CH_2\text{-}CH(CH_3)_2]_2$	49	88	745	80
h	$O\text{-}CH_2\text{-}CH_2\text{-}CH(CH_3)_2$	$N(C_4H_9)_2$	36	—	732	81, 82

[a] Measurement in chloroform

Scheme 2: Preparation of the 1-aryl-3-stilbenylsquaraines **2f–h.**

(Scheme 1). In the first step bromine is exchanged by lithium and then a 1,4-addition of the organometallic compound to the enone **6** takes place. A spontaneous elimination of methanol and subsequent hydrolysis gives the semisquaric acid **8**, which reacts as an electrophile in the aromatic substitution of the anilines **9**. Due to electronic and steric effects the C-3 position of **8** proved to have the highest reactivity, so that the

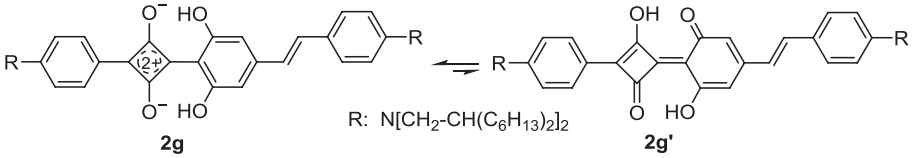

Scheme 3: Resorcinol-derived squaraines such as **2g** do not exist to a perceptible amount in the tautomeric form **2g′**.

squaraines **2a–e** are generated as the major products [75, 76]. The *trans*-configuration of **7** is preserved in the whole process.

The squaraines **2a–e** are high-melting compounds which are poorly soluble in organic solvents. Their absorption maxima in chloroform lie between 614 and 627 nm in the orange region of the visible light so that their solutions are green-blue. The comparison of **2a** to the 1,3-diarylsquaraine **1b** [77, 78], which both bear a dimethylamino and a methoxy group as electron-donating groups, reveals a bathochromic shift of 48 nm for the absorption maximum. This proves, that the effect of extension of conjugation is as predicted – even when the corresponding electronic transition is predominantly localized in the core [63–65].

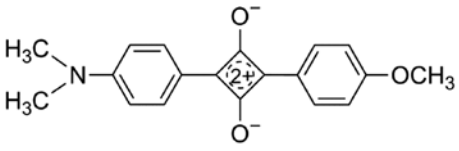

1b (λ_{max} = 579 nm in chloroform)

An alternative synthetic route to 1-aryl-3-stilbenylsquaraines **2** is shown in Scheme 2. The Friedel-Crafts reaction of squaric acid dichloride (**10**) and the benzene derivatives **11** yields after hydrolysis the semisquaric acids **12**, which can be coupled directly to the resorcinol systems **13**. The two hydroxy groups of **13** enhance the nucleophilicity and establish hydrogen bonds in the resulting squaraines **2f–h** [79–82]. Stilbenes without or with just one hydroxy group do not react in this kind of condensation reactions. The mixed solvent 1-butanol/toluene forms an azeotrope with water, which allows to remove continuously the generated water, when the refluxing solvent was previously dried with Na_2SO_4 [77]. The *trans*-configuration of **13** is maintained in the products **2f–h**. The squaraine **2h**, prepared by Marder and coworkers [81], was the very first stilbenoid squaraine.

Due to the long and branched alkyl chains the melting points of **2f–h** are much lower than those of **2a–e** and their solubility in organic solvents is much better. The absorption maximum of **2f**, which has an electron-releasing end group only on one side, lies at 674 nm, whereas **2g** and **2h** (with electron-donating substituents on both sides) exhibit absorption maxima at 745 and 732 nm, respectively.

The comparison of the absorption of **2g** to that of the related 1,3-diarylsquaraine **1c** [80] reveals a strong red-shift of 103 nm to the long-wavelength end of the visible region.

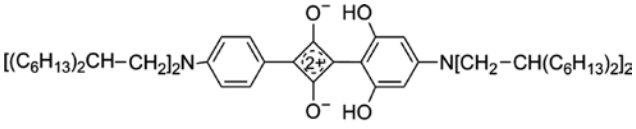

1c (λ_{max} = 642 nm in chloroform)

In principle, the resorcinol structure of **2f–h** enables a tautomeric equilibrium. However, a significant participation of a tautomeric form **2g′** could be ruled out for **2g** (Scheme 3) on the basis of an NMR study of the ^{1}H,^{13}C spin couplings [67].

3 1,3-Distilbenylsquaraines

The direct coupling of semisquaric acids **12** and dihydroxystilbene **13**, shown in Scheme 2 can be applied twice in the condensation reaction of squaric acid (**14**) and two molecules of **15**. The yields of the reaction are low to moderate; however, the process is a very facile one-step reaction (Scheme 4), which is a great advantage in materials science [75, 80, 83–90].

The 1,3-distilbenylsquaraines **3a–s** form dark blue, blue-green or blue-violet crystals. Dissolved in chloroform they show an intense absorption with λ_{max} between 680 and 950 nm. The higher the electron releasing tendency of the terminal substituents is, the more is the band shifted into the NIR region. The extension of the conjugation on both sides of the core has a dramatic effect. The comparison of for example **3q** and **1d**, which have identical donor groups, reveals a red-shift of 244 nm (in chloroform) [88].

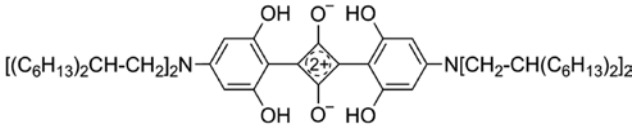

1d (λ_{max}= 657 nm in chloroform)

The unsymmetrical 1,3-distilbenylsquaraines **3t–w** can be obtained by the condensation reaction of dihydroxystilbenes **16** and stilbenylsemisquaric acids **17** (Scheme 5) [67, 75, 76]. The process resembles the synthesis of **2f–h** (Scheme 2).

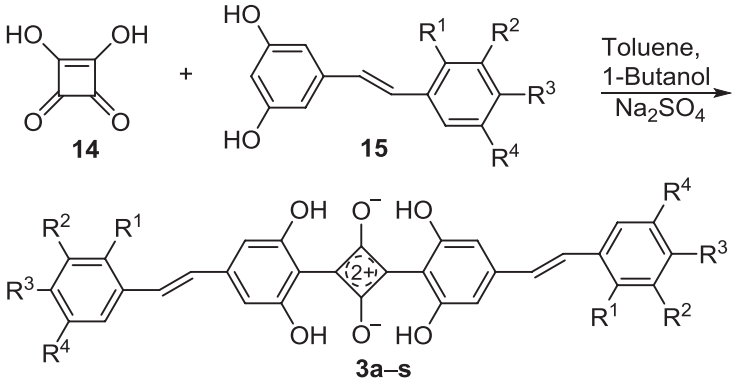

3	R^1	R^2	R^3	R^4	Yield (%)	λ_{max} (nm)	Ref.
a	H	H	OH	H	49	696	83, 84
b	H	H	OC_6H_{13}	H	33	714	75, 83, 84
c	H	H	OC_8H_{17}	H	23	721	75, 83
d	H	H	$OC_{10}H_{21}$	H	9	717	75, 83
e	H	H	$OC_{12}H_{25}$	H	8	719	75, 83
f	H	H	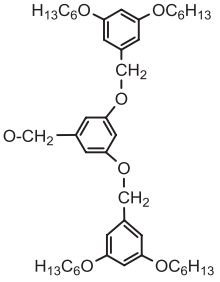	H	8	720	85
g	H	OC_6H_{13}	H	OC_6H_{13}	16	680	83
h	H	OC_6H_{13}	OH	OC_6H_{13}	21	735	75, 83
i	H	OC_6H_{13}	OC_6H_{13}	H	28	730	75, 83, 86
j	H	OC_6H_{13}	OCH_3	OC_6H_{13}	–	–	84
k	H	OC_6H_{13}	OC_6H_{13}	OC_6H_{13}	20	727	83, 84
l	C_6H_{13}	H	H	C_6H_{13}	7	688	80
m	OC_3H_7	H	H	OC_3H_7	4	712	80
n	H	H	$N(C_4H_9)_2$	H	–	–	87
o	H	H	$N(C_6H_{13})_2$	H	13	891	80
p	H	H	$N(CH_2\text{-}CH(C_2H_5)\text{-}C_4H_9$	H	10	894	80
q	H	H	$N[CH_2\text{-}CH(C_6H_{13})_2]_2$	H	13	901	88
r	OC_7H_{15}	H	$N(C_7H_{15})_2$	H	93	942	89, 90
s	$N(C_5H_{11})_2$	H	$N(C_5H_{11})_2$	H	4.5	924	90

Scheme 4: Preparation of the symmetrical 1,3-distilbenylsquaraines **3a–s**.

4 Multiple squaraine chromophores attached to stilbenoid scaffolds

Multiple squaraine dyes can be obtained by two-, three- or fourfold coupling reactions of semisquaric acid **18** with stilbenoid resorcinol derivatives [79]. The reaction conditions are identical to those in Schemes 2 and 4. Bis(2-hexyloctyl)amino groups were used as electron donating and solubilizing substituents. Scheme 6 depicts the reaction of **18** with tetrahydroxystilbene **19** to yield **20a** (22%) [79]. Analogous reactions gave **20b** [81] and **21a** (29%) [79], **21b** (55%) [79], **22** (49%) [79], **23** (20%) [79] and **24** (35%) [79]. Dye **20b** was studied for an application in display front filters [72, 91].

Table 1 summarizes absorption and emission data of the multiple squaraines **20–24** in comparison to the monosquaraine **2f**.

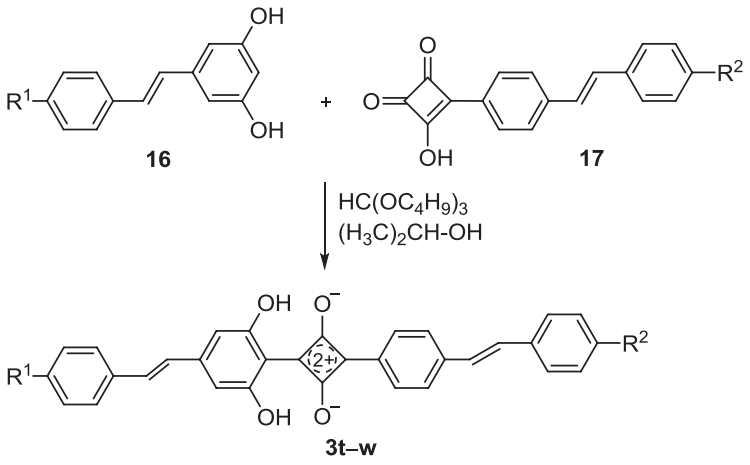

3	R^1	R^2	Yield (%)	λ_{max} (nm) in $CHCl_3$	Ref.
t	$OC_{10}H_{21}$	OC_6H_{13}	13	683	75, 76
u	$N(C_6H_{13})_2$	OC_3H_7	25	781	76
v	$N[CH_2\text{-}CH(C_6H_{13})_2]_2$	OC_3H_7	10	791	76
w	$N[CH_2\text{-}CH(C_6H_{13})_2]_2$	$O\text{-}(CH_2)_6\text{-}OH$	10	790	67

Scheme 5: Preparation of the unsymmetrical 1,3-distilbenyl-squaraines **3t–w**.

The major goal of the investigation of the multiple squaraines was the enhancement of the absorbance. The absorption bands of **20–24** have very different ε_{max} values (Table 1) and very different widths at half height between 552 and 1334 cm^{-1} [79]. Together with the different aggregation tendency, a quantitative comparison with **2f** is difficult. However, the statement that the absorption intensities per squaraine unit of **21a**, **21b**, **22**, **23** and **24** are much higher than that of the model compound **2f** is certainly correct [79]. Conjugation, cross-conjugation and even homoconjugation of squaraine building blocks have obviously an effect on the absorption intensity per squaraine unit.

5 Oligophenylenevinylene (OPV) chains for the extension of conjugation in squaraine dyes

The bathochromic shift observed for the absorptions of 1,3-diarylsquaraines, whose conjugation was extended by styryl building blocks, stimulated activities to study the incorporation of a larger number of 1,4-phenylenevinylene segments. According to the procedure discussed in Scheme 2 the series **1c**, **2g**, **25**, and **26** (Fig. 4) was synthesized by condensation reactions of the corresponding semisquaric acid and a resorcinol of the OPV type [88]. The solubility of the resulting squaraines could be improved by amino groups which bear 2-hexyloctyl substituents [88].

The absorption maximum is bathochromically shifted on going from $n=0$ to $n=1$ ($\Delta\lambda=103$ nm), but then a saturation tendency can be observed for higher n values; λ_{max} reaches a limiting value of 694 ± 2 nm ($n=2, 3$).

The symmetrical series **1d**, **3q**, **27** and **28** ($n=0$–3) with OPV building blocks on both sides was prepared according to Scheme 4 from squaric acid and the corresponding resorcinol derivatives [88]. An analogous process led to the related series **3l**, **29** and **30** ($n=1$–3) without amino substituents as terminal donor groups [80]. The first member **1e** ($n=0$) of this series is still unknown. The different absorption behavior of the two series is interpreted in Section 6.

6 Spectroscopic characterization of stilbenoid squaraines

The distribution of the electron density of the squaraines is characteristically reflected in the ^{13}C chemical shifts of their core units. Whereas the CO groups (C-2 and C-4) of the four-membered rings have fairly constant δ values of 183 ± 2 ppm, the chemical shifts of C-1 and C-3 depend

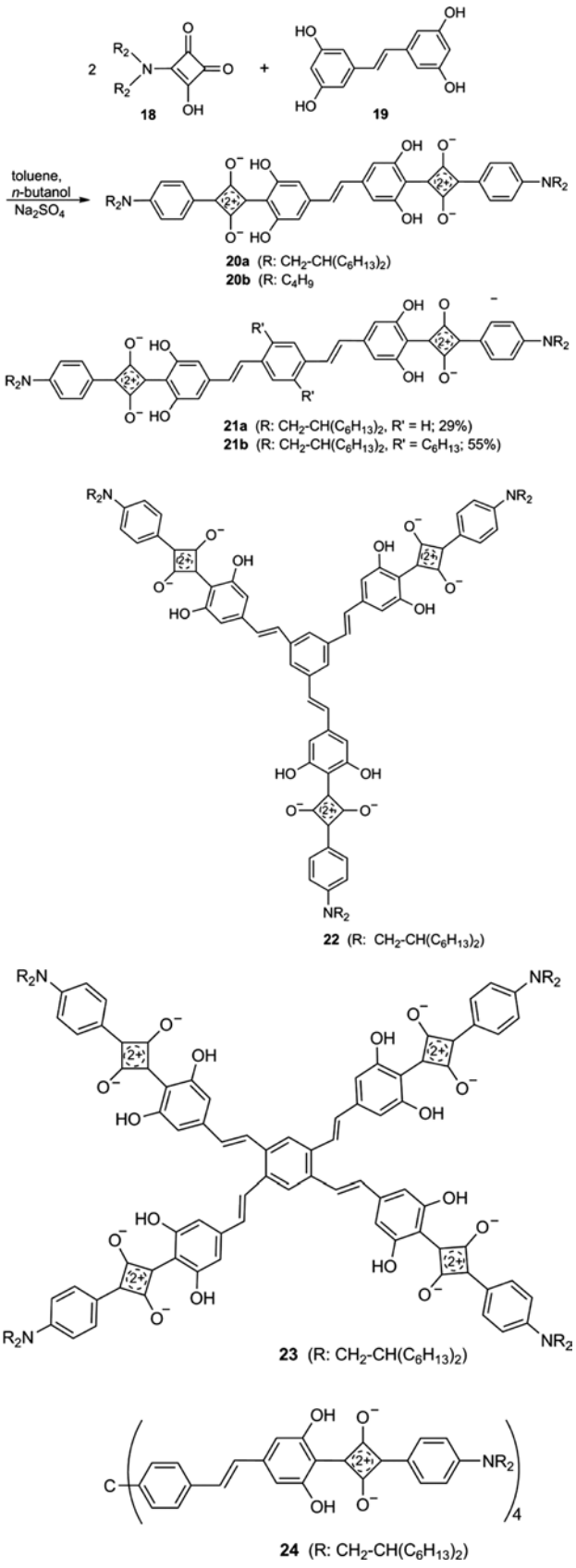

Scheme 6: Preparation of multiple squaraine dyes fixed to stilbenoid scaffolds.

Table 1: Vis/NIR spectroscopic data of the multiple squaraines **20–24** and of the model compound **2f** (measurements in chloroform).

Dye	Number of squaraine units	Absorption λ_{max} (nm)	$10^{-5}\,\varepsilon_{max}$ (L mol^{-1} cm^{-1})	Fluorescence λ_{max} (nm)
2f	1	674	2.70	702
20a	2	778	2.58	798
21a	2	724	4.56	750
21b	2	720	3.34	761
22	3	693	8.11	714
23	4	707	3.93	753
24	4	687	7.23	702

strongly on the nature of the substituents R^i in these positions and vary between 160 and 190 ppm. The higher the partial positive charge in C-1 or C-3 is, the higher is the corresponding δ (^{13}C) value. The different types of squaraines discussed in this article and their ^{13}C chemical shifts are listed in Table 2.

The substituents R^2 take over more of the positive charge of the squaraine core than R^3, and much more than R^1.

The distribution of the electron density along the OPV chain can be traced by the ^{1}H and ^{13}C chemical shifts [92]. Figure 6 shows the comparison of the ^{13}C NMR data of squaraine **3q** and its precursor **15q** for the positions of partial positive charges in **3q**. Down-field shifts can be observed for all these positions. The most pronounced effect is found for the phenylene carbon atom in *p*-position to the squaraine ring ($\Delta\delta = 154.1–141.2 = 12.9$ ppm) and for the olefinic β carbon atom ($\Delta\delta = 137.9–129.8 = 8.1$ ppm).

Orientated at the various potential applications of the squaraine compounds, their most important spectroscopic property concerns the UV/Vis/NIR absorption and emission. Figure 7a shows as an example the spectrum of 1,3-distilbenylsquaraine **3i** in $CHCl_3$ [83]. The long-wavelength band of **3i** is relatively broad and has its maximum at 730 nm. The band arises from the superposition of monomer and aggregate absorptions. The monomer **3i** gives a fluorescence band with a maximum at 787 nm and an excitation spectrum with a maximum at 753 nm. The difference between absorption and excitation spectrum results from H-aggregates of **3i** which do not fluoresce.

The intermolecular interactions of **3i** are even more obvious in the solid state spectrum (Fig. 7b), which shows a panchromatic absorption from the UV far into the NIR region [83].

The long-wavelength bands of squaraines are in many cases a superposition of monomer and aggregate absorptions because squaraines have a high tendency to form

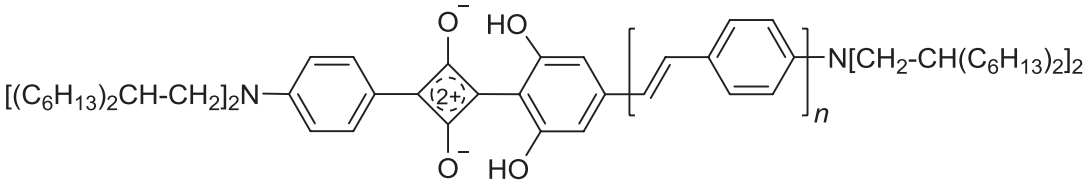

1c (n = 0), **2g** (n = 1), **25** (n = 2), **26** (n = 3)

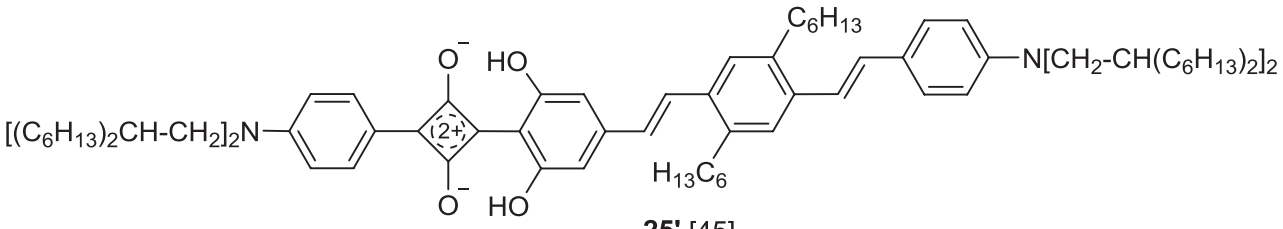

25' [45]

Comp.	n	Yield (%)	λ_{max} (nm) in $CHCl_3$
1c	0	48	642
2g	1	49	745
25	2	34	692
25'	2	49	695
26	3	35	696

Fig. 4: 1,3-Diarylsquaraines with OPV chains on one side, and the model compound **1c**.

Table 2: ^{13}C Chemical shifts (δ values in ppm) of C-1 and C-3 in the squaraine rings bearing the substituents R^i (i = 1–3); measurements in $CDCl_3$).

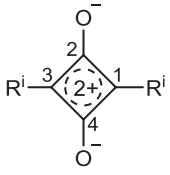

1–R^i / 3–R^i	**R^1** 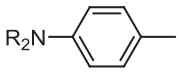	**R^2** 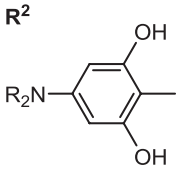	**R^3** 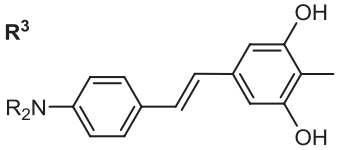
R^1	C—1 187 ± 4 C—3 187 ± 4	C—1 164 ± 8 C—3 179 ± 8	C—1 174 ± 3 C—3 179 ± 3
R^2		C—1 161 ± 5 C—3 161 ± 5	unknown
R^3			C—1 169 ± 4 C—3 169 ± 4

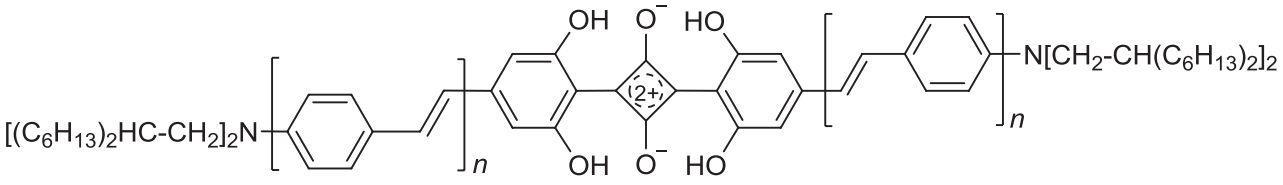

1d (*n* = 0), **3q** (*n* = 1), **27** (*n* = 2), **28** (*n* = 3)

Comp.	*n*	Yield (%)	λ_{max} (nm) in $CHCl_3$
1d	0	36	657
3q	1	13	901
27	2	26	816
28	3	11	736

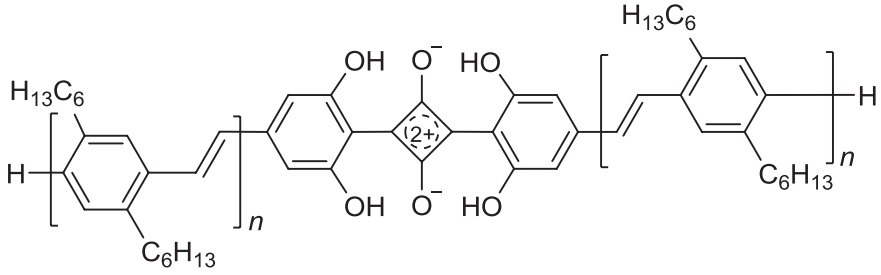

1e (*n* = 0), **3l** (*n* = 1), **29** (*n* = 2), **30** (*n* = 3)

Fig. 5: Series of squaraines bearing OPV chains on both sides, and the model compounds **1d** and **1e**.

H- and J-aggregates [68, 69, 92]. The individual squaraine structure, the solvent, the concentration and the temperature determine the type of aggregate and its stability.

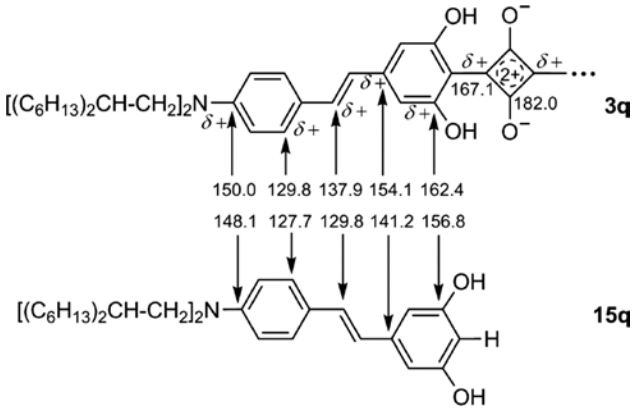

Fig. 6: Comparison of the ^{13}C chemical shifts of the 1,3-distilbenylsquaraine **3q** and the corresponding resorcinol **15q** for the positions bearing a partial positive charge in **3q** (measurements in $CDCl_3$ at room temperature) [88].

Figure 8 shows the absorption of 1,3-distilbenylsquaraine **3o** [85] dissolved in *n*-heptane at a total concentration of about 10^{-5} mol L^{-1}. At least four absorbing species can be recognized. Addition of dichloromethane leads to a strong band, whose maximum is red-shifted by 140 nm. It can be assigned to the monomer, because highly diluted solutions in *n*-heptane ($c \leq 10^{-6}$ mol L^{-1}) show only this band.

The conclusion has been supported by a temperature-dependant measurement in acetonitrile (Fig. 9). Raising the temperature from 35 to 60°C leads to the decrease of absorptions of H- and J-aggregates and to a strong increase of the absorption of the monomer at λ_{max} to 815 nm [85].

The solvent dependence of the absorption of 1,3-distilbenylsquaraine **3q** [85] at room temperature is presented in Table 3: λ_{max} varies between 835 and 909 nm. The correlation of λ_{max} with the solvent parameters E_T (30) [93] is very crude (Fig. 10) [74, 85]. Different aggregates in equilibria with the monomers exist in solvents with different polarity. Obviously, chlorine containing solvents (numbers 5, 7 and 8 of the list) give rise to absorption maxima at particularly low wavenumbers (large wavelengths). Solvents

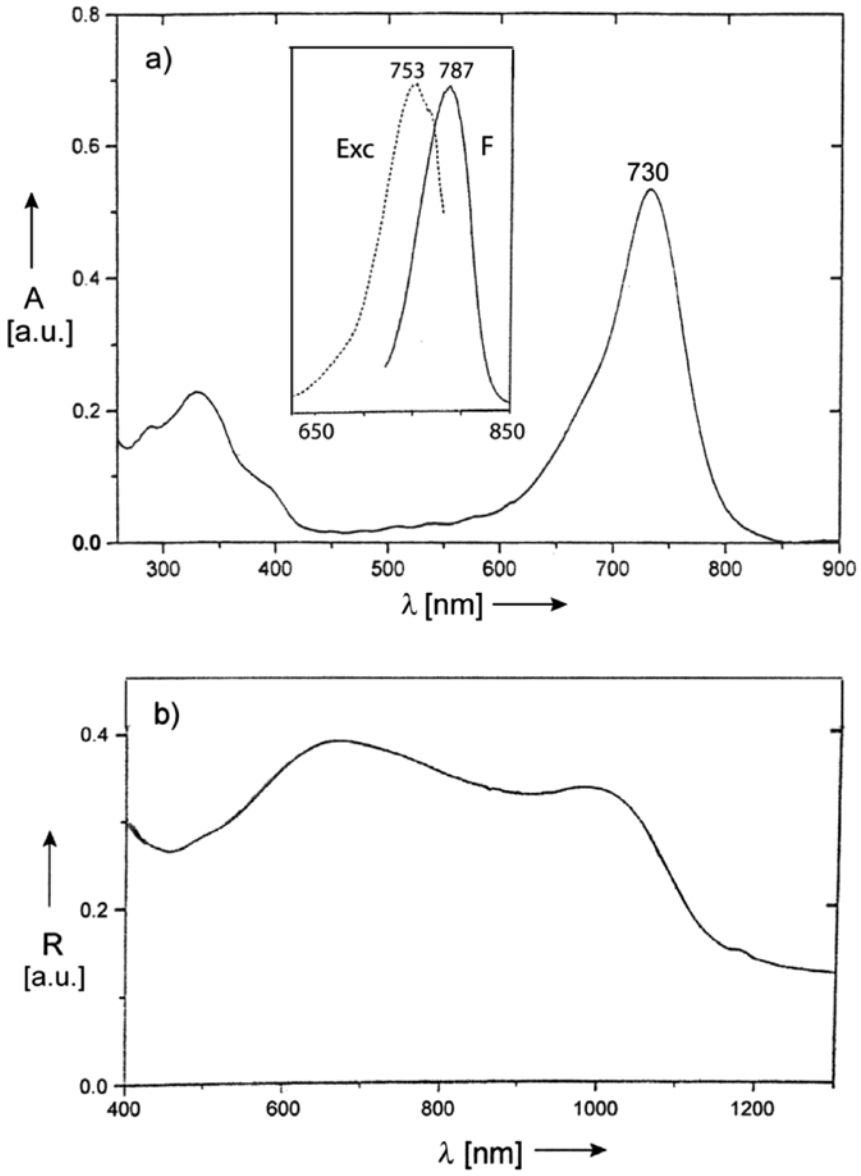

Fig. 7: (a) UV/Vis/NIR spectrum of 1,3-bis(4-{2-[3,4-bis(hexyloxy)-phenyl]ethenyl}-2,6-dihydroxyphenyl)squaraine (**3i**) in $CHCl_3$. The insert exhibits the fluorescence and the excitation spectrum in $CHCl_3$; (b) solid-state reflection measurement of a dispersion of **3i** in a not specified silane matrix.

with a high nucleophilicity can attack on the squaraine core and destroy the dye.

The UV/Vis/NIR absorption of squaraines bearing OVP chains deserves special attention. The wavelengths of the absorption maxima exhibit first a bathochromic shift for the extension of conjugation (*n*: 0→1) in the unsymmetrical series **1c**, **2g**, **25**, **26** (Fig. 4) as well as in the symmetrical series **1d**, **3q**, **27**, **28** (Fig. 5). However, further extension of the conjugation (*n*: 1→2, 3) leads then to a hypsochromic shift in both series. This effect represents a typical behavior of series of conjugated oligomers bearing very strong terminal donor and acceptor groups [70]. The amount of intramolecular charge transfer (ICT) decreases when the distance between D and A becomes larger and the increasing length of the conjugated arm A-π-D cannot compensate that. Increasing conjugation and decreasing ICT have an opposite effect on λ_{max} in organic solvents (Fig. 11). When the terminal amino groups are protonated, they lose their donor character. The original structure D-π-A-π-D adopts an A-π-A-π-A character, and a continuously bathochromic shift to a limiting value for high numbers *n* can be observed in this series [70].

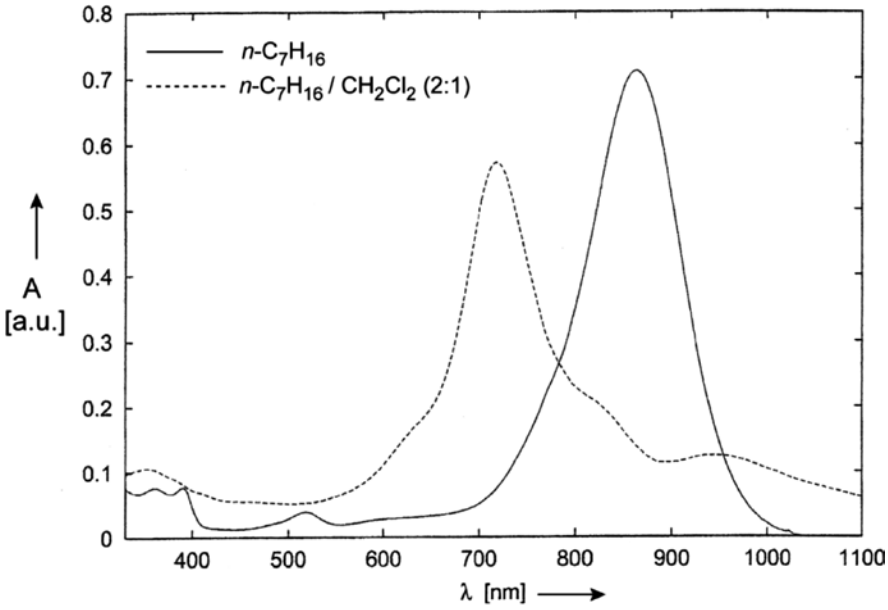

Fig. 8: UV/Vis/NIR spectrum of 1,3-bis{4-[2-(4-dihexylaminophenyl) ethenyl]-2,6-dihydroxyphenyl}squaraine (**3o**) in an apolar and a partly polar solvent.

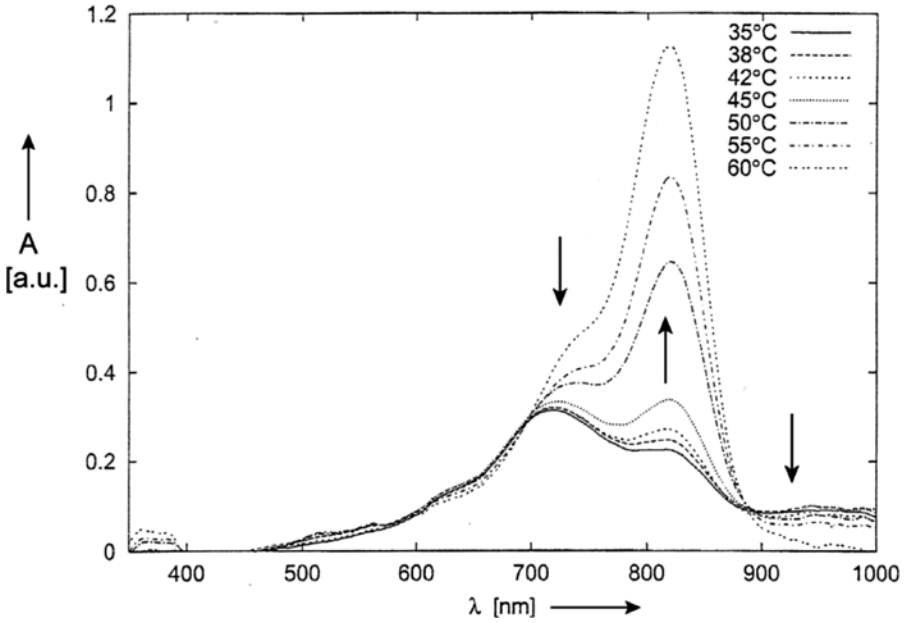

Fig. 9: UV/Vis/NIR absorption spectra of **3o** in acetonitrile at different temperatures.

The squaraine series **1e**, **3l**, **29**, **30** has OPV chains without terminal donor groups and behaves as observed for many series of conjugated oligomers, and also for the protonated series introduced above: an increasing number n gives rise to a bathochromic shift increasing to a limiting value λ_∞. The first member of the series, 1,3-bis(2,6-dihydroxyphenyl)squaraine (**1e**) is an unknown compound. On the basis of the data for the isomeric compound 1,3-bis(2,4-dihydroxyphenyl)squaraine ($\lambda_{max} = 567$ nm) and for 1,3-bis(2,4,6-trihydroxyphenyl) squaraine ($\lambda_{max} = 563$ nm) a λ_{max} value of 565 ± 5 nm can be estimated for **1e** and its aggregates [69, 94].

Table 3: Solvent dependence of the UV/Vis/NIR absorption of 1,3-distilbenyl-squaraine **3q**.

Solvent	E_T (30) (kcal mol^{-1})	Absorption λ_{max} (nm)	$\tilde{\nu}_{max}$ (cm^{-1})
1 Cyclohexane	30.9	843	11,862
2 *n*-Heptane	31.3	835	11,976
3 Toluene	33.9	846	11,820
4 1,4-Dioxane	36.0	848	11,792
5 1,1,1-Trichloroethane	36.2	894	11,186
6 Tetrahydrofuran	37.4	879	11,377
7 Chloroform	39.1	901	11,099
8 Dichloromethane	40.7	909	11,001
9 Acetone	42.2	890	11,236

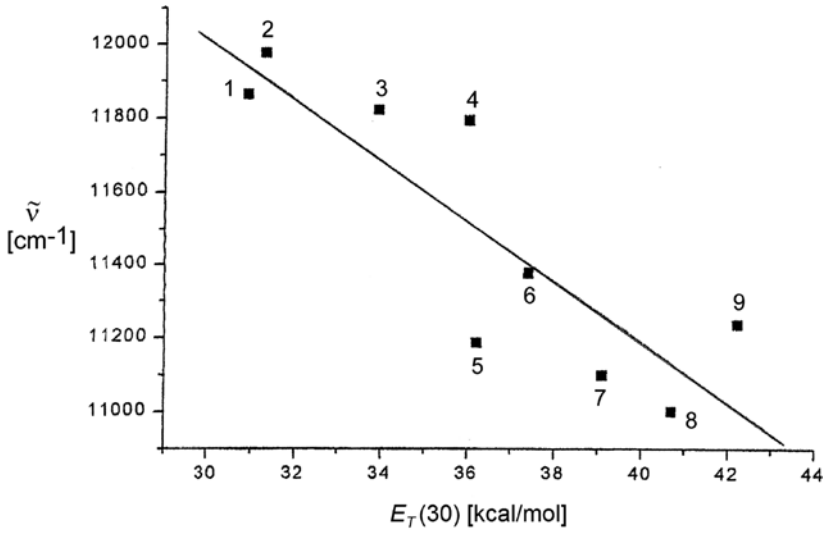

Fig. 10: Correlation of the absorption maximum of 1,3-bis[4-(2-{4-[bis(2-hexyloctyl)amino]phenyl}ethenyl)-2,6-dihydroxyphenyl]squaraine (**3q**) in nine different solvents (see Table 3) with the E_T(30) parameters.

7 Conclusion

Squaraines have the character of biradicaloid donor-acceptor-donor (D-π-A-π-D) compounds, whose absorption and emission can be bathochromically shifted into the NIR region, when the π-conjugation in one or both branches A-π-D is extended from phenyl to stilbenyl groups. Further extension to oligo(1,4-phenylenevinylene) chains (OPV) has the contrary effect for systems bearing strong terminal donor groups, because the intramolecular charge-transfer (ICT) between donor D and acceptor A is impaired by the increasing distance of A and D.

For optimum performance, *trans*-stilbene building blocks, present e. g. in 2,6-dihydroxy-4-[2-(4-dialkylaminophenyl)-ethenyl]phen-1-yl groups, are best suited, because the hydroxyl groups guarantee a more perfect planarity by intramolecular hydrogen bonds and because they carry additional electron donor groups. Amino groups bearing long branched alkyl chains such as 2-hexyloctyl ensure a fairly good solubility in di- or trichloromethane.

The absorption intensity of such squaraine dyes and their often present H- and/or J-aggregates is high and can still be enhanced, when two to four arylsquaraine units are attached to give conjugated, cross-conjugated or homo-conjugated stilbenoid scaffolds.

All the squaraines presented in this article can be readily synthesized (Schemes 1, 2, 4–6). The series of dihydroxyphenyl compounds for example can be obtained by the direct condensation reaction of a dihydroxystilbene derivative and squaric acid. The easy access together with the strong absorption and fluorescence in the Vis/NIR region renders the stilbenoid squaraine dyes promising candidates for many applications in materials science.

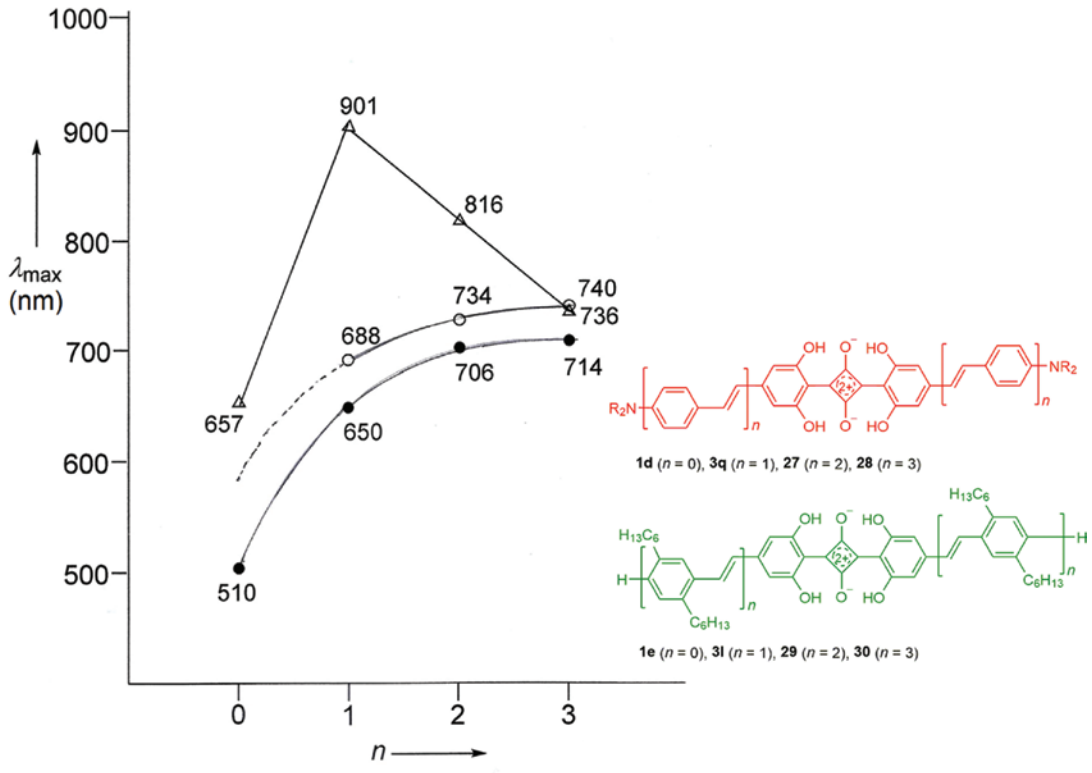

Fig. 11: Absorption maxima of different squaraine series: Δ: **1d**, **3q**, **27**, **28** ($n = 0–3$) in $CHCl_3$; •: **1d** · H^+, **3q** · H^+, **27** · H^+, **28** · H^+ ($n = 0–3$) in $CHCl_3$-CF_3COOH; o: **3l**, **29**, **30** ($n = 1–3$) in $CHCl_3$.

References

[1] A. Treibs, K. Jacob, *Angew. Chem., Int. Ed. Engl.* **1965**, *4*, 694.
[2] W. Ziegenbein, H. E. Sprenger, *Angew. Chem., Int. Ed. Engl.* **1966**, *5*, 893.
[3] A. H. Schmidt in *Oxocarbons*, (Ed.: R. West), Academic Press, New York, **1980**, p. 185.
[4] S. Das, K. G. Thomas, M. V. George, *Mol. Supramol. Photochem.* **1997**, *1*, 467.
[5] K.-Y. Law, *Mol. Supramol. Photochem.* **1997**, *1*, 519.
[6] A. Ajayaghosh, *Acc. Chem. Res.* **2005**, *38*, 449.
[7] B. Halton, *Chem. N. Z.* **2008**, *72*, 57.
[8] Z. Chen, A. Lohr, C. R. Saha-Möller, F. Würthner, *Chem. Soc. Rev.* **2009**, *38*, 564.
[9] L. Beverina, P. Salice, *Eur. J. Org. Chem.* **2010**, *2010*, 1207.
[10] L. D. Patsenker, A. L. Tatarets, O. P. Klochko, E. A. Terpetschnig, *Springer Ser. Fluoresc.* **2010**, *9*, 159.
[11] L. D. Patsenker, A. L. Tatarets, E. A. Terpetschnig, *Springer Ser. Fluoresc.* **2010**, *8*, 65.
[12] R. R. Avirah, D. T. Jayaram, N. Adarsh, D. Ramalah, *Org. Biomol. Chem.* **2012**, *10*, 911.
[13] L. Yuan, W. Lin, K. Zheng, L. He, W. Huang, *Chem. Soc, Rev.* **2013**, *42*, 622.
[14] J. Roncali, P. Leriche, P. Blanchard, *Adv. Mater.* **2014**, *26*, 3821.
[15] L. Beverina, M. Sassi, *Synlett* **2014**, *25*, 477.
[16] M. Gsänger, D. Bialas, L. Huang, M. Stolte, F. Würthner, *Adv. Mater.* **2016**, *28*, 3615.
[17] A. Broggi, H. Kim, J. Jung, M. P. Bracciale, M. L. Santarelli, C. Kim, A. Marrocchi, *Macromol. Chem. Phys.* **2017**, *218*, 1600487.
[18] H.-W. Lin, Y.-C. Shiau, U.S. 9871217 B1 20180116, **2018**.
[19] V. Maltese, S. Cospito, A. Beneduci, B. C. De Simone, N. Russo, G. Chidichimo, R. A. J. Janssen, *Chem. Eur. J.* **2016**, *22*, 10179.
[20] Q. Xiao, S. Yang, R. Wang, Y. Zhang, H. Zhang, H. Zhou, Z. Li, *Dyes Pigm.* **2018**, *154*, 137.
[21] Q.-J. Sun, G.-F. Dong, H.-Y. Zheng, H.-Y. Zhao, J. Qiao, L. Duan, L.-D. Wang, F.-S. Zhang, Y. Qiu, *Wuli Huaxue Xuebao* **2011**, *27*, 1893.
[22] U. Mayerhöffer, K. Deing, K. Gruss, H. Braunschweig, K. Meerholz, F. Würthner, *Angew. Chem. Int. Ed. Engl.* **2009**, *48*, 8776.
[23] R. Bisht, V. Sudhakar, K. Mele, F. Munavvar, N. Jarjule, J. Nithyanandhan, *ACS Appl. Mater. Interfaces* **2018**, *10*, 26335.
[24] Q. Xiao, F. Wu, M. Han, Z. Li, L. Zhu, Z. Li, *J. Mat. Chem. A*, **2018**, *6*, 13644.
[25] H.-C. Zhu, C.-F. Li, Z.-H. Fu, S.-S. Wei, X.-F. Zhu, J. Zhang, *Appl. Surf. Sci.* **2018**, *455*, 1095.
[26] V. Punitharasu, K. Mele, F. Munavvar, J. Nithyanandhan, *ACS Appl. Mater. Interfaces* **2018**, *10*, 16541.
[27] Y. Haishima, Y. Kubota, K. Manseki, J. Jin, Y. Sawada, T. Inuzuka, K. Funabiki, M. Matsui, *J. Org. Chem.* **2018**, *83*, 4389.
[28] G. M. Paterno, N. Barbero, S. Galliano, C. Barolo, G. Lanzani, F. Scotognella, R. Borrelli, *J. Mat. Chem. C* **2018**, *6*, 2778.
[29] J. Wu, C. Si, Y. Chen, L. Yang, B. Hu, G. Chen, Z. Lu, Y. Huang, *Chem. Eur. J.* **2018**, *24*, 3234.
[30] Y. Chen, G. Wang, L. Yang, J. Wu, F. S. Melkonyan, Y. Huang, Z. Lu, T. J. Marks, A. Facchetti, *J. Mat. Chem. C* **2018**, *6*, 847.
[31] Z. Li, S. Xu, Y. Du, *Appl. Mech. Mater.* **2011**, *80–81*, 360.

[32] G. J. Ashwell, J. Ewington, K. Moczko, *J. Mat. Chem*. **2005**, *15*, 1154.
[33] M. Yang, S. Li, J. Ma, Y. Jiang, *Chem. Phys. Lett*. **2002**, *354*, 316.
[34] L. Beverina, M. Crippa, P. Salice, R. Ruffo, C. Ferrante, I. Fortunati, R. Signorini, C. M. Mari, R. Bozio, A. Facchetti, G. A. Pagani, *Chem. Mater*. **2008**, *20*, 3242.
[35] H. Abrahamse, M. R. Hamblin, *Biochem. J*. **2016**, *473*, 347.
[36] T. Liu, X. Liu, Y. Zhang, M. V. Bondar, Y. Fang, K. D. Belfield, *Eur. J. Org. Chem.* **2018**, *2018*, 4095.
[37] B. Wu, Y. Lin, B. Li, C. Zhan, F. Zeng, S. Wu, *Analyt. Chem*. **2018**, ahead of print.
[38] S. Khopkar, S. Deshpande, G. Shankarling, ACS *Sustainable Chem. Eng*. **2018**, *6*, 10798.
[39] K. Strassel, A. Kaiser, S. Jenatsch, A. C. Veron, S. B. Anantharaman, E. Hack, M. Diethelm, F. Nüsch, R. Aderne, C. Legnani, S. Yakunin, M. Cremona, R. Hany, *ACS Appl. Mater. Interfaces* **2018**, *10*, 11063.
[40] T. S. Jarvis, F. M. Roland, K. M. Dubiak, P. W. Huber, B. D. Smith, *J. Mat. Chem. B* **2018**, *30*, 4963.
[41] G. Wang, W. Xu, H. Yang, N. Fu, *Dyes Pigm.* **2018**, *157*, 369.
[42] S. K. Shaw, C. L. Schreiber, F. M. Roland, P. M. Battles, S. P. Brennan, S. J. Padanilam, B. D. Smith, *Bioorg. Med. Chem.* **2018**, *26*, 2085.
[43] J. Gayton, L. McNamara, A. Huckaba, T. Rill, E. Sharpe, S. Autry, N. Hammer, J. Delcamp, Abstracts of Papers, 255th ACS National Meeting & Exposition, New Orleans, LA (USA) March 18–22, **2018**, ORGN-292.
[44] S. Dong, J. D. W. Teo, L. Y. Chan, C.-L. K. Lee, K. Sou, *ACS Appl. Nano Mater.* **2018**, *1*, 1009.
[45] W. Liu, A. Johnson, B. D. Smith, *J. Am. Chem. Soc*. **2018**, *140*, 3361.
[46] M. Saikiran, D. Sato, S. S. Pandey, S. Hayase, T. Kato, *Bioorg. Med. Chem. Lett.* **2017**, *27*, 4024.
[47] G. Saranya, P. Anees, M. M. Joseph, K. K. Maiti, A. Ajayaghosh, *Chem. Eur. J*. **2017**, *23*, 7191.
[48] M. Shimi, V. Sankar, M. K. A. Rahim, P. R. Nitha, S. Das, K. V. Radhakrishnan, K. G. Raghu, *Chem. Commun*. **2017**, *53*, 5433.
[49] G. Wang, W. Xu, Y. Guo, N. Fu, *Sens. Actuators B* **2017**, *245*, 932.
[50] M. Ptaszek, *Progr. Mol. Biol. Transl. Sci.* **2013**, *143*, 59.
[51] I. C. Wu, J. Yu, F. Ye, Y. Rong, M. E. Gallina, B. S. Fujimoto, Y. Zhang, Y.-H. Chan, W. Sun, X.-H. Zhou, C. Wu, D. T. Chiu, *J. Am. Chem. Soc*. **2015**, *137*, 173.
[52] D. Shangguan, Y. Wei, X. Liu, L. Shen, X. Zhang, T. Bing, Faming Zhuanli Shenquing CN 108070275, **2018**.
[53] I. Miletto, A. Fraccarollo, N. Barbero, C. Barolo, M. Cossi, L. Marchese, E. Gianotti, *J. Chem. Soc., Dalton Trans*. **2018**, *47*, 3038.
[54] M. S. Soumya, D. Gayathri Devi, K. M. Shafeekh, S. Das, A. Abraham, *Photodiagn. Photodyn. Ther.* **2017**, *18*, 302.
[55] P. S. S. Babu, P. M. Manu, T. J. Dhanya, P. Tapas, R. N. Meera, A. Surendran, K. A. Aneesh, S. J. Vadakkancheril, D. Ramaiah, S. A. Nair, M. R. Pillai, *Sci. Rep.* **2017**, *7*, 42126.
[56] A. H. Schmidt, *Synthesis* **1980**, 961.
[57] C. G. Krishna, L. P. Avinash, K. Bhanuprakash, *RSC Adv.* **2015**, *5*, 18813.
[58] A. L. Puyad, C. Prabhakar, K. Yesudas, K. Bhanuprakash, V. J. Rao, *J. Mol. Struct. Theochem*. **2009**, *904*, 1.
[59] K. Srinivas, C. Prabhakar, C. L. Devi, K. Yesudas, K. Bhanuprakash, V. J. Rao, *J. Phys. Chem. A* **2007**, *111*, 3378.
[60] A. L. Puyad, G. K. Chaitanya, C. Prabhakar, K. Bhanuprakash, *J. Mol. Model*. **2013**, *19*, 275.
[61] K. Yesudas, G. K. Chaitanya, K. Bhanuprakash, V. J. Rao, *J. Phys. Chem. A* **2006**, *110*, 11717.
[62] K.-Y. Law, F. C. Bailey, *Canad. J. Chem*. **1993**, *71*, 494.
[63] H. Ozawa, K. Yoshiro, S. Yabushita, *Chem. Phys. Lett*. **2015**, *625*, 78.
[64] C. Cornelissen-Gude, W. Rettig, R. Lapouyade, *J. Phys. Chem. A* **1997**, *101*, 9673.
[65] R. W. Bigelow, H.-J. Freund, *Chem. Phys*. **1986**, *107*, 159.
[66] I. B. Burgess, P. Rochon, N. Cunningham, *Opt. Mater*. **2008**, *30*, 1478.
[67] H. Meier, 2019, unpublished work.
[68] A. Kaczmarek-Kedziera, D. Kedziera, *Theor. Chem. Acc*. **2016**, *135*:214 and references therein.
[69] S. Das, T. L. Thanulingam, K. G. Thomas, P. V. Kamet, M. V. George, *J. Phys. Chem*. **1993**, *97*, 13620.
[70] H. Meier, *Angew. Chem. Int. Ed*. **2005**, *44*, 2482.
[71] H. Meier, M. Lehmann in *Encycl. Nanosci. Nanotechnol.*, (Ed.: H. S. Nalwa), Vol. 10, American Scientific Publishers, Stevensons Ranch **2004**, p. 95.
[72] N. Sekine, K. Ookuba, PCT Int. Appl. WO 2008035554 A1 20080327, **2008**.
[73] S. Ohira, I. Rudra, K. Schmidt, S. Barlow, S.-J. Chung, Q. Zhang, J. Matichak, S. R. Marder, J.-L. Bredas, *Chem Eur. J*. **2008**, *14*, 11082.
[74] See however: D. Keil, H. Hartmann, *Dyes Pigm*. **2001**, *49*, 161.
[75] H. Meier, U. Dullweber, *Tetrahedron Lett*. **1996**, *37*, 1191.
[76] H. Meier, R. Petermann, U. Dullweber, *J. Prakt. Chem./Chem. Ztg*. **1998**, *340*, 744.
[77] K.-J. Law, F. C. Bailey, *J. Org. Chem*. **1992**, *57*, 3278.
[78] F. Meyers, C.-T. Chen, S. R. Marder, J.-L. Bredas, *Chem. Eur. J.* **1997**, *3*, 530.
[79] J. Gerold, U. Holzenkamp, H. Meier, *Eur. J. Org. Chem*. **2001**, *2001*, 2757.
[80] J. Gerold, Doctoral Thesis, University of Mainz, Mainz, **2001**.
[81] C. T. Chen, S. R. Marder, L. T. Cheng, *J. Am. Chem. Soc*. **1994**, *116*, 3117.
[82] S. R. Marder, C. T. Chen, L. T. Cheng, US 5500156A 19960319, **1996**.
[83] H. Meier, U. Dullweber, *J. Org. Chem*. **1997**, *62*, 4821.
[84] J. H. Banning, J. W. Thomas, Jr. B. Wu, S. V. Drappel, Ger. Offen. DE 102014216684 A1 20150226, **2015**.
[85] R. Petermann, *Doctoral Thesis*, University of Mainz, Mainz, **2001**.
[86] N. Takiguchi, PCT Int. Appl. WO 2017110511 A1 20170629, **2017**.
[87] Y. Hirai, D. Sasaki, Y. Jimbo, PCT Int. Appl. WO 2017043175 A1 20170316, **2017**.
[88] H. Meier, R. Petermann, J. Gerold, *Chem. Commun*. **1999**, *1999*, 977.
[89] R. Petermann, M. Tian, S. Shinura, M. Furuki, Jpn. Kokai Tokkyo Koho JP 2004067892 A 20040304, **2004**.
[90] R. Petermann, M. Tian, S. Tatsuura, M. Furuki, *Dyes Pigm*. **2003**, *57*, 43.
[91] N. Sekine, K. Ookubo, Kokai Tokkyo Koho 2009 JP 2009040860 A 20090226, **2009**.
[92] Y. Xu, Z. Li, A. Malkovsky, S. Sun, Y. Pang, *J. Phys. Chem. B* **2010**, *114*, 8574.
[93] C. Reichardt, *Solvents and Solvent Effects in Organic Chemistry*, VCH, Weinheim, **1988**, p. 365.
[94] S. Rosselli, D. Danner, Z. A. Bamedi, G. Nelles, T. Miteva, G. Fuhrmann, PCT Int. Appl. WO 2016120166 A1 20160804, **2016**.